Membrane Water Treatment, *Vol. 6, No. 5 (2015) 393-409*
DOI: http://dx.doi.org/10.12989/mwt.2015.6.5.393

Membrane behavior of bentonite-amended compacted clay towards Zn(II) and Pb(II)

Qiang Tang *[1], Takeshi Katsumi[2], Toru Inui[2] and Zhenze Li[3]

[1] *School of Urban Rail Transportation, Soochow University, China*
[2] *Graduate School of Global Environmental Studies, Kyoto University, Japan*
[3] *Department of Civil Engineering, University of Ottawa, Canada*

(*Received January 14, 2015, Revised May 28, 2015, Accepted July 02, 2015*)

Abstract. Zinc and lead pollution are public environmental issues that have attracted lots of attention for a long time. Landfill leachate contains heavy metals, such as Zn(II) and Pb(II), which are usually related to the pollution of groundwater, especially in developing countries. Bentonite has been proven to be effective in enhancing the membrane property of clay, by which landfill liners can have better barrier performance towards the migration of contaminants. In this study, 5% sodium bentonite amended with locally available Fukakusa clay was utilized to evaluate the membrane behavior towards the heavy metals zinc and lead. The chemico-osmotic efficiency coefficient, ω, was obtained through Zn(II) and Pb(II) solutions with different concentrations of 0.5, 1, 5, 10, and 50 mM. According to the results, ω continually decreased as the Zn(II) and Pb(II) concentrations increased, which is consistent with the Gouy-Chapman theory. Compared to normal inorganic ions, the membrane behavior towards heavy metal ions was lower. The migration of heavy metal ions was not observed based on experimental results, which can be attributed to the adsorption or ion exchange reaction. The mechanisms of the membrane performance change were discussed with the assistance of XRD patterns, free swelling results, XRF results, and SEM images.

Keywords: Bentonite amended compacted clay; Zn(II); Pb(II); membrane behavior; adsorption; mechanism

1. Introduction

Because of the rapid development of industrial economies, the environment is faced with severe heavy metal pollution. These metals are discharged into the environment in numerous ways, including from mine drainage, car manufacturing, painting, smelters and metal refineries, and industrial and domestic sewage (Kimbrough and Suffer 1995). Unlike organic pollutants, which are susceptible to biological degradation, heavy metals are not biodegradable and sometimes such pollution may last for two millennia (Hong *et al.* 1994). What is worse, heavy metals tend to accumulate in biological systems and can result in severe environmental problems; they can even threaten people’s health.

Zinc is an essential trace nutrient that is required by most living organisms for healthy growth and enzyme function (Tang *et al.* 2012). However, it is toxic to plants and animals at elevated

---

*Corresponding author, Ph.D., E-mail: tangqiang@suda.edu.cn

ISSN: 2005-8624 (Print), 2092-7037 (Online)

concentrations. Lead is a common contaminant and even a little has the potential to cause chronic diseases and brain damage in humans (Tang *et al*. 2009). Therefore, the maximum concentration limits for Zn(II) and Pb(II) in drinking water have been strictly regulated. For example, the Canadian Water Quality Guidelines (2004) and Indian Standard (1991) recommend that the concentration of Zn(II) in drinking water not exceed 5 mg/L; the WHO recommends 3 mg/L as an upper limit for Zn(II) and 0.01 mg/L for Pb(II) (WHO 2006). The U.S. Environmental Protection Agency (2011) also proposed risk-based drinking water criteria, which recommended that the concentration of Zn(II) not exceed 5 mg/L and that the concentration of Pb(II) should be lower than 0.015 mg/L.

Landfilling remains the predominant treatment method for the disposal of municipal solid waste (MSW) around the world. According to Baun and Christensen (2004), most landfill leachates contain concentrations of Zn(II) up to 155 mg/L and Pb(II) up to 1.5 mg/L. In an effort to prevent the groundwater pollution caused by the diffusion of landfill leachates, developing affordable and efficient barriers, like compacted clay used as bottom liners in landfill facilities, has attracted more attention in the past several years (Shelley and Daniel 1993, Chapuis 2002). And bentonite has proven to possess excellent membrane behavior and can thus greatly enhance the barrier's performance (Kang and Shackelford 2010, Shackelford 2012).

Membrane behavior in clay, by which the liners can restrict the migration of selected substances while allowing the passage of water (like a semipermeable membrane), is usually characterized based on two factors: size restriction and static electro-repulsion from a diffuse double layer (Van Impe 2002). Typically the degree that soil acts as a membrane is quantified in terms of the chemico-osmotic efficiency coefficient, ω (Mitchell 1993, Malusis and Shackelford 2002, Manassero and Dominijanni 2003). ω ranges from 0 to 1 ($0 \leq \omega \leq 1$), where 0 represents no solute restrictions and 1 represents an ''ideal'' or ''perfect'' membrane that completely restricts the movement of solutes (Kemper and Rollins 1966, Olsen 1969, Barbour and Fredlund 1989, Keijzer *et al*. 1997).

Extensive researches have reported various factors that influence membrane behavior, e.g., the mineralogy of clay, solute type, concentration, pH, and consolidation process (Malusis and Shackelford 2002, Van Impe 2002, Kang and Shackelford 2010, 2011). However, very few researches have evaluated membrane behavior towards heavy metals. The compacted clay liner, especially when applied as landfill bottom liners, will have direct exposure to landfill leachate, sometimes with a very high concentration of heavy metals, especially in hazardous material landfill sites. Thus, the objective of this study is to evaluate membrane behavior towards the heavy metals Zn(II) and Pb(II) in different concentrations. Based on experiment results, the mechanisms of the membrane performance change are discussed with the assistance of XRD patterns, free swelling results, XRF results, and SEM images.

2. Materials and experimental method

2.1 Soils and solutions

The materials employed in this study were: (1) locally available natural clay known as Fukakusa clay (FC) obtained from Kyoto, Japan; and (2) commercial sodium bentonite, originally from Wyoming, U.S. and purchased from Hojun Co. Ltd. Table 1 lists select physical and chemical properties of Fukakusa clay and bentonite (Tang *et al*. 2014).

Table 1 Properties of Fukakusa clay and bentonite

Property	Unit	Standard	Values	
			Fukakusa clay	Bentonite
Soil particle density	g/cm^3	JIS A 1202	2.717	2.635
Natural water content	%	JIS A 1203	3.7	6.5
Soil pH		ASTM D 4972-01	3.0	9.7
Swell index	mL/2g-solid	ASTM D 5890-06	3.0	23.0
Plastic limit	%	JIS A 1205	14	47.3
Liquid limit	%	JIS A 1205	53	540
Cation exchange capacity	meq/100g	JGS 0261-2009	14.9	56.1
Exchangeable metals	meq/100g	ASTM D7503-10		
Ca			10.5	22.1
Mg			3.8	13.8
Na			0.6	43.7
K			2.2	1.8
Sum			17.1	81.3
Soluble salts	mg/kg	ASTM D7503-10		
Ca			1578	664
Mg			798	1210
Na			578	7423
K			108	195
Chemical composition		JIS M 8853		
SiO_2	%		49.3	66.1
Fe_2O_3	%		20.4	21.6
Al_2O_3	%		13.6	4.2
CaO	%		2.2	3.8
K_2O	%		6.9	1.7
TiO_2	%		2.4	0.8
ZrO_2	%		0.2	0.2
SrO	%		0.1	0.2
MnO	%		0.2	0.2
Grain size distribution		JIS A 1204		
Sand fraction	%		30.1	
Silt fraction	%		53.7	
Clay fraction	%		16.2	
Uniformity coefficient			29.1	
Coefficient of curvature			2.2	

De-ionized water and various concentrations of $ZnCl_2$ and $Pb(NO_3)_2$ solutions were used in this study. De-ionized water (DIW) was prepared from tap water by using a water distillation apparatus (RFD240NA, Advantec, Japan). Zinc chloride and lead nitrate (guaranteed reagent, Wako Ltd., Japan) were dissolved in DIW, then diluted to target concentrations of 0.5, 1, 5, 10, and 50 mM.

Table 2 Measured chemical properties of the solutions

Liquid	Concentration		pH	EC (mS/m) @ 18 °C
	(mM)	(mg/L)		
De-ionized water	0	0	6.8	0.2
$ZnCl_2$ solutions	0.5	68	6.3	10
	1	136	6.5	19.7
	5	680	6.5	92.8
	10	1360	6.3	184
	50	6800	6.1	867
$Pb(NO_3)_2$	0.5	166	6.2	13.92
	1	331	5.8	26.7
	5	1655	5.7	117
	10	3310	5.7	199
	50	16550	5.3	863

The pH and electrical conductivity (EC) of the above solutions were measured by a pH/ion/cond.-meter (F-55, Horiba, Japan); the results are shown in Table 2.

2.2 Membrane test apparatus and procedures

The membrane test apparatus applied in this study is shown in Fig. 1; it is the same as the one used in Tang *et al*. (2015). The specimen was locked inside the cylinder by a top cap and base pedestal to maintain constant thickness. Porous stones cover both sides to prevent clogging. Ports were equipped and connected with pipes and peristaltic tube pumps (SMP-23AS, as one, Japan), respectively, at both sides to form two independent circulation loops. The pressure transducer (PTI-S-JC300-22AQ-T, Swagelok, Germany) was installed at the top side to measure the actual chemico-osmotic pressure.

Fukakusa clay was mixed with 5% bentonite following the optimum water content 23.2%, as measured in Tang *et al*. (2014). After stirring for 10 minutes (KM-800, Kenmix, Japan), the sample was covered with a polyethylene membrane and allowed to stand for 12 hours to ensure the water was well distributed.

The specimens were prepared in three stages: assembly, saturation, and flushing. First, each sample was compacted by three layers directly in the column for a later membrane test with an inner diameter of 100 mm and height of 30 mm following ASTM D698-12. Then, all the specimens were submerged into DIW inside a vacuum chamber connected to a pump (LMP100, Welch, Japan) for saturation for one day. After that, specimens were permeated with DIW with the hydraulic gradient around 135 for flushing, which was to remove soluble salts from the specimens in order to enhance the potential of the membrane behavior (Kang and Shackelford 2009, 2011). During the flushing stage, the outflow volume, duration, and hydraulic gradient were recorded for use in the hydraulic conductivity calculation following Darcy’s law.

Before each membrane test, DIW was circulated over both the top and bottom surfaces at a constant circulation rate (about 205 mL/day) for six days to establish a steady baseline pressure prior to introducing different concentration solutions. The membrane tests consisted of five

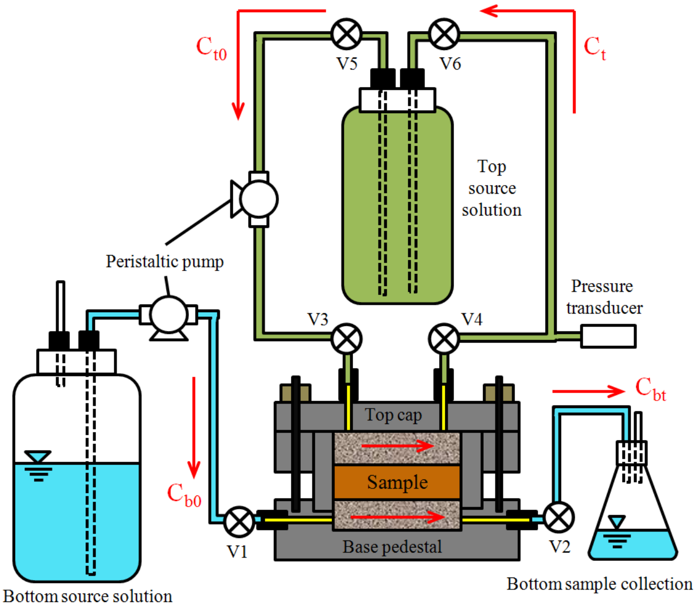

Fig. 1 Test apparatus for membrane test

individual stages. In each stage, one of the five electrolytes with $ZnCl_2$ or $Pb(NO_3)_2$ in concentrations of 0.5, 1, 5, 10, and 50 mM was infused sequentially into the top porous stone of the specimen, while the bottom surface was kept flushing with DIW. The solution at the top of the specimens represented the leachate of a landfill, while the flushing boundary at the bottom represented the aquifer underneath. The concentration in the leachate is generally higher than in the groundwater; therefore, a concentration difference was expected to appear across the liner (Dominijanni and Manassero 2012a). Each stage of the test was conducted until a stable chemico-osmotic pressure across the specimen was observed. The circulation loop at the bottom provided outflow for sample collection to measure concentration of Zn(II) and Pb(II) by AAS (AA-6800, SHIMADZU, Japan), and EC and pH were measured twice per day. To improve the reliability of the test results, the experiments were carried out in a room with a control temperature of 18 ± 1°C.

2.3 Calculation of membrane efficiency

Throughout the membrane tests, the thickness and volume remained constant, and the infused liquid was equal to the outflow, which was to prevent the source solution and DIW from entering or exiting the specimens. The chemico-osmotic efficiency coefficient ω was defined as follows (Katchalsky and Curran 1965, Groenevelt and Elrick 1976, Van *et al.* 1996, Malusis and Shackelford 2002)

$$\omega = \frac{\Delta P}{\Delta \pi} \tag{1}$$

Where ΔP is the actual chemico-osmotic pressure across the specimen and $\Delta \pi$ is the theoretical chemico-osmotic pressure across an ideal semi-permeable membrane (Olsen *et al.* 1990). For a single salt system, $\Delta\pi$ can be approximated using the van't Hoff equation based on the solution concentration difference as follows (Katchalsky and Curran 1965, Metten 1966, Tinoco *et al.* 1995)

$$\Delta\pi = vRT\Delta C \tag{2}$$

Where v is the number of ions in one salt molecule; R is the universal gas constant, 8.314 J/mol·K; T represents the absolute temperature of the membrane testing system in K; and ΔC is the concentration difference across the specimen, which can be rewritten as follows (Malusis and Shackelford 2002)

$$\Delta C = (C_t - C_b) \tag{3}$$

Where C_t and C_b represent solute concentration at the top and bottom sides, respectively. In this study, the source solution was circulated at the top surface to provide an initial upper concentration of $C_{t0} > 0$, while the bottom surface was flushed by DIW to make a bottom concentration of $C_{b0} \approx 0$. Thus, the chemico-osmotic efficiency coefficient, ω_0, in terms of the KCl solution, can be expressed as follows (Malusis and Shackelford 2002)

$$\omega_0 = \left.\frac{\Delta P}{\Delta\pi}\right|_0 = \frac{\Delta P}{\Delta\pi_0} = \frac{\Delta P}{vRT\Delta C_0} = \frac{\Delta P}{vRT(C_{t0} - C_{b0})} = \frac{\Delta P}{2RTC_{t0}} \tag{4}$$

Where $\Delta\pi_0$ exists under a undary KCl concentrations caused by diffusion are negligible. However, in practice, the diffusion and insufficient circulation rate at the bottom sides may result in a time-dependent reduction of $\Delta\pi$ (Malusis *et al.* 2001). Thus, the average chemico-osmotic efficiency coefficient ω_{ave} was more accurate in describing the actual membrane behavior, which can be written as follows (Kang and Shackelford 2009)

$$\omega_{ave} = \left.\frac{\Delta P}{\Delta\pi}\right|_{ave} = \frac{\Delta P}{\Delta\pi_{ave}} = \frac{\Delta P}{vRT\Delta C_{ave}} = \frac{\Delta P}{2RT(C_{t,ave} - C_{b,ave})} \tag{5}$$

Where $C_{t,ave}$ and $C_{b,ave}$ are the average KCl concentrations across the top and bottom, respectively, of the specimen boundaries.

3. Results

3.1 Specimen flushing

Figs. 2(a)-(c) presents the flushing stage; the results are summarized in Table 3. The flushing stage lasted for 70 days, until the EC of outflow was lower than 3.6 mS/m and the pH was close to 7.0 (neutral). From Table 3, the initial EC of outflow were 810 and 695 mS/m, which are almost 150-200 times higher than the target value. With continual permeation with DIW, the EC of outflow decreased gradually and eventually reduced to 3.5 and 2.8 mS/m, respectively. According to flushing progress, to make outflow pH much closer to 7.0 through flushing, perhaps one or two more months are required, as shown in Fig. 2(b). To reduce the total duration of the membrane test, the flushing stage was stopped after the outflow pH of the two specimens increased to 6.0 and 5.9, respectively.

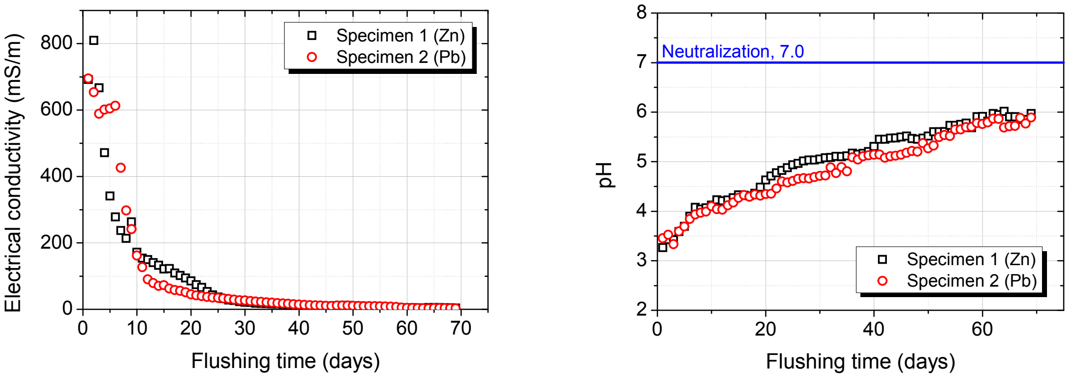

(a) EC (b) pH values

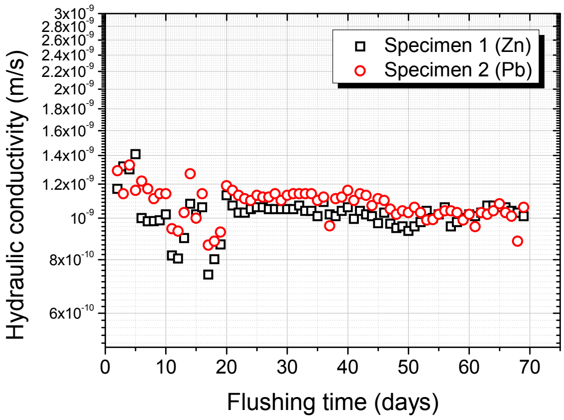

(c) Hydraulic conductivities

Fig. 2 Specimens' flushing

Table 3 EC, pH and hydraulic conductivity (*k*) before and after flushing

No.		1 (Zn)	2 (Pb)
Specimen	Unit	FC+5% Bentonite	FC+5% Bentonite
Flushing stage start			
EC	mS/m	810	695
pH		3.1	3.5
k	m/s	$1.17 \text{ x } 10^{-9}$	1.29×10^{-9}
Flushing stage terminate			
EC	mS/m	3.5	2.8
pH		6.0	5.9
k	m/s	$0.98 \text{ x } 10^{-9}$	0.99×10^{-9}

*Flushing method: constant head; Duration: 70 days; Hydraulic gradient: 135

Fig. 2(c) presents the measured hydraulic conductivities of the two specimens towards DIW during the flushing stage. Compared to the initial one, the hydraulic conductivities slightly decreased with time, which was also observed by Tang *et al.* (2014). This time-dependent decrease was attributed to the concentration decrease of leaching flow during the flushing stage (Tang *et al.* 2014). And according to Shackelford *et al.* (2000), lower concentration results in lower hydraulic conductivity. After 70 days of flushing, the hydraulic conductivities gradually stabilized at around 0.98×10^{-9} m/s and 0.99×10^{-9} m/s, which already reach the requirement of the upper limit of hydraulic conductivity for direct landfill liners (Kamon and Katsumi 2001, Katsumi *et al.* 2008a).

3.2 Boundary results during the membrane tests

Figs. 3(a)-(b) show the top and bottom boundary concentrations during the membrane tests. The tests consisted of five stages where in the Zn(II) and Pb(II) concentrations for the top circulation increased from 0.5 mM to 50 mM. It was apparent that Zn(II) and Pb(II) concentrations inside the top circulation decreased greatly ($C_t < C_{t0}$), especially during the first two stages, in which the concentration of solute decreased almost to 0.The decrease in concentration at the top side can be attributed to diffusion and adsorption (Tang *et al.* 2009, 2012). In the first two stages, almost all Zn(II) and Pb(II) was absorbed by the soil at the top surface of the specimens, and the soil at the top surface reached the adsorption capacity as the solute concentration continually increased. That the concentrations of Zn(II) and Pb(II) still decreased at relatively high concentrations can be attributed to the fact that more heavy metal ions diffused to the deeper places. Compared to the decreased concentration at the top side, at the bottom side the concentration remained stable ($C_t \approx C_{t0}$). Such a phenomenon appeared because the Zn(II) and Pb(II) were absorbed by surrounding soil minerals when transported across the specimens.

Figs. 4(a)-(b) present the boundary pH values during the membrane tests. The pH values at the top side decreased after every stage, which also indicated the occurrence of adsorption and diffusion. Thus, some acidic salts originated from the ion-exchange adsorption or leached out from the specimen since the diffusion process resulted in a decrease in pH values. In the case of pH at the bottom side, the obvious decrease trends can be observed at the beginning of the first stage (0.5 mM) and the final two stages at concentrations of 10 and 50 mM. A similar phenomenon was also

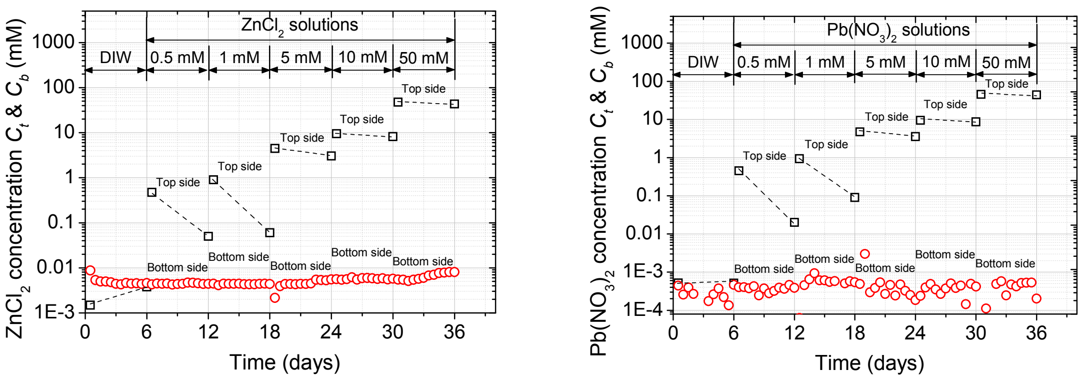

(a) $ZnCl_2$ (b) $Pb(NO_3)_2$

Fig. 3 Boundary concentrations during membrane test

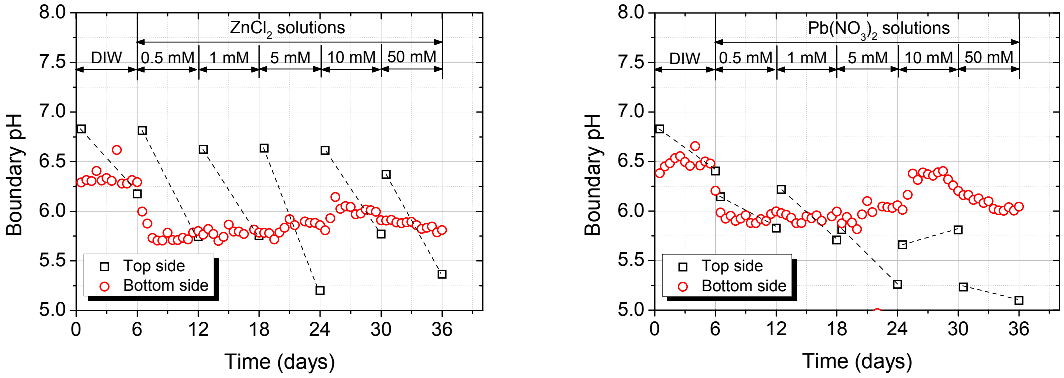

(a) ZnCl$_2$ (b) Pb(NO$_3$)$_2$

Fig. 4 Boundary pH values during membrane test

observed by Tang *et al*. (2014) and attributed to the leaching out of acidic substances originating from diffusion and ion-exchange adsorption.

3.3 Chemico-osmotic pressure

Figs. 5(a)-(b) show the actual values of ΔP for the two specimens. DIW was circulated at both the top and bottom sides of the specimens ($C_t = C_b = 0$) during the first six days to obtain the baseline pressures 0.93 kPa and 0.59 kPa. The baseline pressures were also observed by Tang *et al*. (2014) and Malusis and Shackelford (2002). Tang *et al*. (2014) ascribed this to the leaching out of the remaining soluble salts in specimens, while according to Malusis and Shackelford (2002) it was due to slight differences in the hydraulic resistance of the porous stones at the opposite ends of the specimens.

From the figures, it is apparent that the introduction of electrolytes resulted in an immediate and rapid increase in the chemico-osmotic pressure. The distinctive change in chemico-osmotic

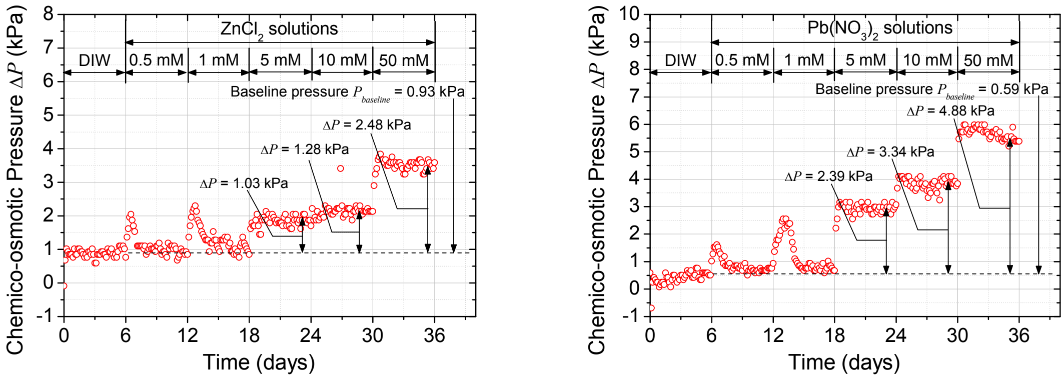

(a) ZnCl$_2$ (b) Pb(NO$_3$)$_2$

Fig. 5 Measured osmotic pressure across the specimens during the membrane tests pressure appeared in Zn(II) and Pb(II) concentrations of 0.5 mM and 1 mM, in which the chemico-osmotic pressure increased greatly to a peak, then decreased until the baseline pressure value was reached or at least neared. Considering the pH condition, such a phenomenon can be attributed to the adsorption process, by which the heavy metal ions were absorbed, resulting in the decrease in concentration difference (Tang *et al.* 2010). Therefore, the chemico-osmotic pressure decreased to the baseline pressure value since all heavy metal ions were absorbed and the concentration difference decreased to zero. After the soil at the top surface of the specimen reached the maximum adsorption capacity, the stable chemico-osmotic pressure was observed at a concentration of 5 and 10 mM. For the Pb(II) at concentration of 50 mM, the chemico-osmotic pressure was still decreasing, which might be due to the adsorption inside the specimen since the solute diffused into the deeper place at a relatively high concentration.

4. Discussions

The comparison of boundary concentrations at the bottom side during the membrane tests are displayed in Fig. 6. In Fig. 6(a), it is clear that the concentration of Pb(II) of the outflow at the bottom side stayed stable; no apparent increase could be observed during the membrane test. It also indicated that Pb(II) cannot transport across the specimens. However, in the case of Zn(II), when the concentration difference reached 50 mM, the diffused Zn(II) was observed across the specimen. Additionally, the EC of outflow for both Zn(II) and Pb(II) increased when the concentration difference increased to 50 mM as shown in Fig. 6(b). Compared to the stable concentration of Zn(II) and Pb(II) at outflow, the increase of EC can be attributed to the ion-exchange adsorption; some soluble salts were also generated. And the EC of outflow for Zn(II) was a little higher than for Pb(II), which resulted from the diffusion of some Zn(II). Compared to the EC for K ions measured by Tang *et al.* (2014), both Zn(II) and Pb(II) were very low, which suggests that K is more active and hard to fix during the diffusion process.

Table 4 presents the membrane test results. The chemico-osmotic efficiency coefficient ω_0 and average chemico-osmotic efficiency coefficient ω_{ave} decreased as the concentration difference increased. Because of the occurrence of adsorption in the first two stages, the average concentration

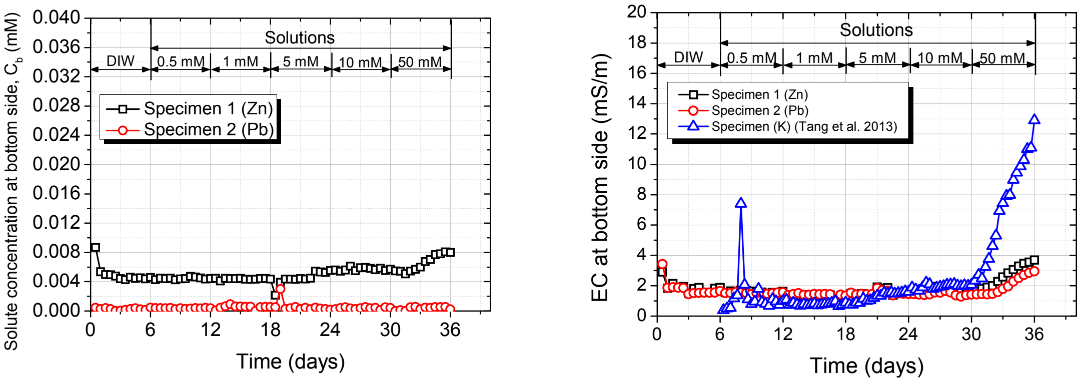

(a) Solute concentration of outflow

(b) EC of Outflow

Fig. 6 Compare of boundary condition of outflow at bottom side during membrane test

Table 4 Summary of the membrane tests results

	Experiment conditions					Membrane test results					
	D (cm)	*T* (cm)	*S* (%)	*k* (m/s)	Solute type	C_t mM	ΔP (kPa)	$\Delta\pi$ (kPa)	$\Delta\pi_{ave}$ (kPa)	ω_0	ω_{ave}
1	10	3	97.7	0.98×10^{-9}	Zn	0.5		3.6		0.33	
						1		7.21		0.19	
						5	1.03	36.04	27.01	0.03	0.04
						10	1.28	72.08	63.75	0.02	0.02
						50	2.48	360.4	327.6	0.01	0.01
2	10	3	95.7	0.99×10^{-9}	Pb	0.5		3.6		0.28	
						1		7.21		0.27	
						5	2.39	36.04	29.69	0.07	0.08
						10	3.34	72.08	65.34	0.05	0.05
						50	4.88	360.4	322.9	0.01	0.02

**D* = Diameter of specimens; *T* = Thickness of specimens; *S* = Saturation degree;
k = hydraulic conductivities; C_t = upper boundary concentration; ΔP = Measured osmotic pressure;
$\Delta\pi$ = theoretical chemico-osmotic pressure; $\Delta\pi_{ave}$ = Average theoretical chemico-osmotic pressure;
ω_0 = Chemico-osmotic efficiency coefficient; ω_{ave} = Average chemico-osmotic efficiency coefficient

difference cannot be obtained; thus, the average chemico-osmotic efficiency coefficient ω_{ave} in the first two stages for Zn(II) and Pb(II) cannot be calculated. As shown in Table 4, because of the continual solute diffusion from the source solution into the specimen and adsorption at top side($C_{t,ave} < C_{t0}$), as well as soluble salts from the specimen to flushing DIW at bottom side ($C_{b,ave} > C_{b0}$), the initial theoretical chemico-osmotic pressure $\Delta\pi$ is slightly higher than the average chemico-osmotic pressure $\Delta\pi_{ave}$, which resulted in the values of ω_{ave} tending to be slightly larger than ω_0 (Malusis *et al.* 2001). Additionally, the difference between the values of ω_{ave} and ω_0 tends to become smaller as the circulating KCl concentration increases (Tang *et al.* 2014).

In Fig. 7, the values of ω_{ave} calculated in this study are compared with that of previous literature for Nelson Farm Clay (NFC) and sodium bentonite presented by Kang and Shackelford (2010) and Malusis and Shackelford (2002). It has to be mentioned that since the average chemico-osmotic efficiency coefficient ω_{ave} for Zn(II) and Pb(II) under 0.5 and 1 mM were not obtained, in order to compare with previous results, the two spots for them in this figure were substituted by ω_0. Although the relative positions of the lines differed with each other, the general trends were the same. Membrane behaviors ω_{ave} decreased as concentration increased, which can likely be attributed to two reasons: the diffuse double layer (DDL) and inter-particle pores (Van Impe 2002).

Bentonite minerals consist of tetrahedral and octahedral layers that provide many hydration sites due to their crystal lattice structure (Yong *et al.* 2010). According to Katsumi *et al.* (2007), the water-bounded molecules are immobile and behave like a solid phase to obstruct the passage of solutions. As the immobile water phase becomes thicker with an increase in bound water molecules, the effective pore space for free flow reduces. However, when the solution's concentration increases, more exchange sites at the DDL are occupied by cations instead of water molecules, causing a stronger attraction force between the soil particle and its DDL. Thus, the inter-layer space becomes narrower, which leads to a decrease in DDL thickness. According to Sposito (1984), the hydration shell surrounding the cations in a DDL consists of about six water molecules for dilute solutions, but this figure falls to about three water molecules in concentrated solutions. According to the Gouy-Chapman theory (DDL theory), the thickness of the DDL decreases as the solute concentration increases, which leads to the increase in inter-particle pore size (Mitchell 1993, Malusis and Shackelford 2002). Thus, it is rational to explain the decrease of membrane behavior as a solute concentration increase.

Yaroshchuk (1995) provided an explanation of the correlation between membrane behavior and the DDL. According to Yaroshchuk (1995), the properties of macroscopic liquid inside the porous medium are determined by the mechanisms caused by interaction between the solid skeleton and the liquid components at the microscopic scale, such as the effect of the DDL (Yaroshchuk 1995, Dominijanni and Manassero 2012b). The state variables of an electrolyte solution are

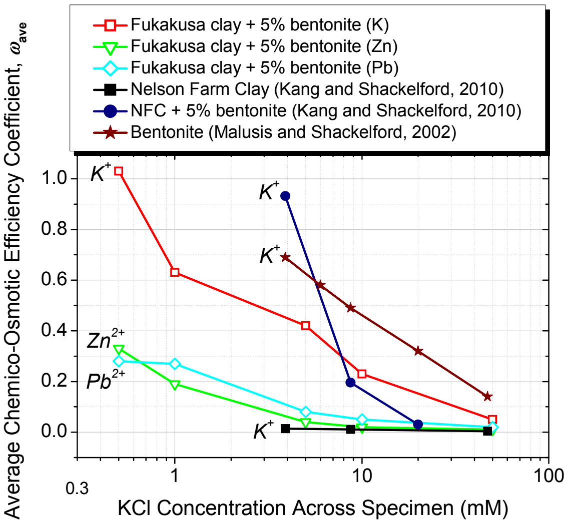

Fig. 7 Chemico-osmotic efficiency coefficient ω_{ave} as function of concentration

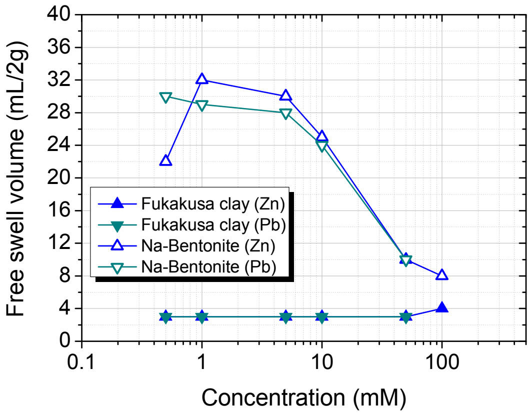

Fig. 8 Free swell of Fukakusa clay and bentonite towards Zn(II) and Pb(II)

discontinuous between the bulk and the pore solution, a phenomenon that is called the partition effect (Yaroshchuk 1995). The partition effect suggests that the inter-particle pore system is independent and that the migration of solute inside is dominated by micro-mechanisms, including the effect from the DDL (Yaroshchuk 1995, Dominijanni and Manassero 2012b).

Katsumi *et al*. (2008b) thought that bentonite could not swell sufficiently inside the electrolyte solution and that the increase in inter-particle pores would allow more solute to pass, which is also attributed to the decrease in membrane behavior at elevated concentrations. Consistent with Katsumi *et al*. (2008b), it can be found that the free swelling volume of bentonite decreases as the solute concentration increases, as shown in Fig. 8. Compared with the sodium bentonite used in this study, the Fukakusa clay possesses almost no swelling property under Zn(II) and Pb(II) conditions.

Fig. 9 shows Scanning Electron Microscope (SEM) (JSM-5510LV, JEOL, Japan) images at the top side of specimens after the membrane tests. Figs. 9(a)-(b) were results concluded from this study, while (c) was cited from Tang *et al*. (2014) for comparison. From the image, it is apparent that the size of soil clusters significantly differed. The average size of soil clusters under the Zn(II) condition was only 5-10 μm and 10-15 μm for Pb(II), while almost 30 μm for K. This indicates that heavy metal ions can cause greater shrinkage to the soil clusters, and compared to K, some

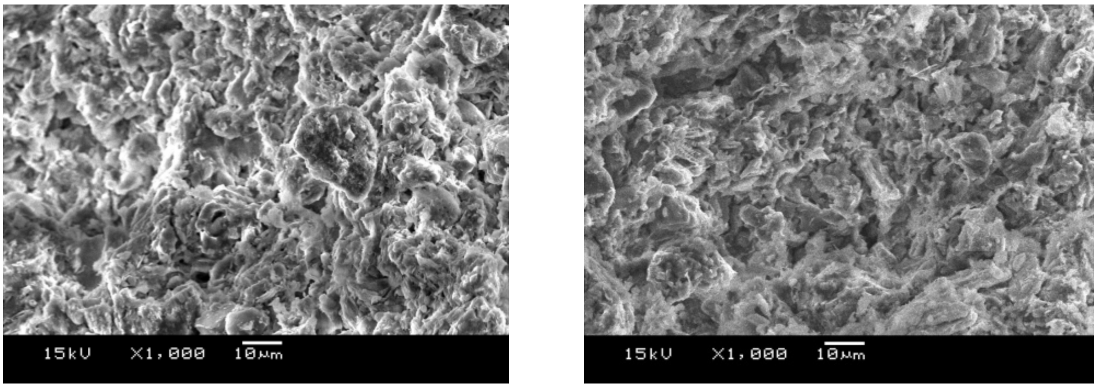

(a) Zn (b) Pb

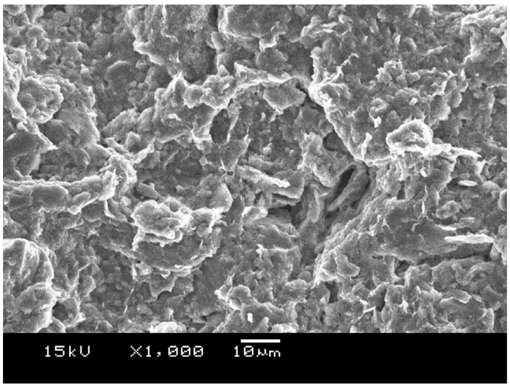

(c) K

Fig. 9 SEM images of the specimens after membrane test

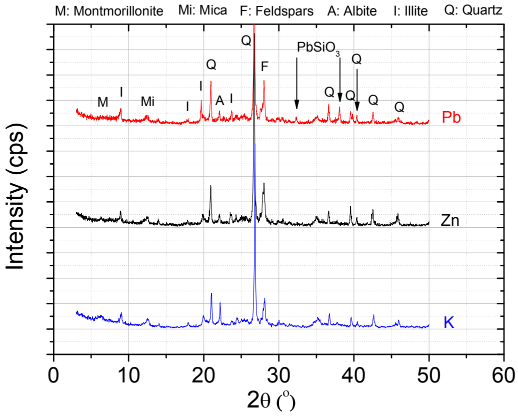

Fig. 10 X-ray diffraction patterns of the samples after membrane test

observable pores also appeared at the surface of the specimens under Zn(II) and Pb(II), which was the permeable path during the diffusion. Therefore, it can be said of the relative position of the average chemico-osmotic efficiency coefficient ω_{ave} that K >Pb> Zn, as shown in Fig. 7.

Although the average chemico-osmotic efficiency coefficient ω_{ave} towards K was much higher than those under Zn(II) and Pb(II), K traveled across the specimen much faster, as shown in Fig. 6(b), which can be attributed to adsorption. To further study the mechanism, X-ray diffraction (RAD-2B, Rigaku Corporation, Japan) was used to help analyze the specimen after the membrane tests, as shown in Fig. 10. The characteristic peak 2θ = 6.42° represents the presence of Montmorillonite, and the weak intensity indicated the limit amount (5% by dry weight). Mica (2θ = 12.48°), illite (2θ = 8.96°, 17.92°, 19.68°, 23.72°), quartz (2θ = 20.98°, 26.78°, 36.68°, 39.6°, 40.38°, 42.6° and 45.94°) and feldspar (2θ = 28.04°) were also found.

Based on XRD patterns, for specimens under the Pb(II) condition, two characteristic peaks appeared at 2θ = 32.36° and 38.10°,which can be identified as $PbSiO_3$. Tang *et al.* (2010) thought that quartz was likely to hydrolyze to form SiO32- ions. Thus, it can help to explain the origin of $PbSiO_3$ as follows

$$\mathrm{SiO_2 + H_2O \rightarrow SiO_3^{2-} + H^+} \tag{6}$$

$$\mathrm{SiO_3^{2-} + Pb^{2+} \rightarrow PbSiO_3(s)\downarrow} \tag{7}$$

Since the generated $PbSiO_3$ in Eq. (7) was a stable compound, it was rational to predict that this reaction would end once all Pb(II) was adsorbed or the soil reached the maximum adsorption capacity, which was also proven by the top boundary concentration as shown in Fig. 3(b). Compared to that under the K condition, the intensity of the characteristic peak, which represents albite at 2θ = 22.10°, under the Zn(II) and Pb(II) conditions were a little weak. Considering the pH condition around 5.0, the albite might be expected to hydrolyze and to form quartz (SiO_2). This hypothesis can also be proven by the intensity of the quartz, which did not become weak after Eqs. (6) and (7).

Because of the pH condition at the top circulation during the membrane test, Pb(II) may be in the form of $Pb(OH)^+$; the existence of lead hydroxide indicates the following precipitation reaction (Tang *et al.* 2009)

$$\mathrm{Pb}^{2+} + \mathrm{H_2O} \rightarrow \mathrm{Pb(OH)}^{+} + \mathrm{H}^{+} \tag{8}$$

$$\mathrm{Pb}^{2+} + \mathrm{H_2O} \rightarrow \mathrm{Pb(OH)_2(s)} \downarrow + \mathrm{H}^{+} \tag{9}$$

The above Eq. (8) can be proven by Table 2 in that the Pb(II) solution exhibited an acidic nature. Additionally, Eq. (9) can help to explain the reason that the pH value always decreased at the end of every stage in Fig. 4(b). Tang *et al.* (2012) refers to the other possible reaction to help explain the adsorption of Zn(II)

$$\mathrm{SiO_2} + \mathrm{H_2O} \rightarrow \mathrm{SiO_4^{4-}} + \mathrm{H}^{+} \tag{10}$$

$$\mathrm{SiO_4^{4-}} + \mathrm{Zn}^{2+} \rightarrow \mathrm{Zn_2SiO_4(s)} \downarrow \tag{11}$$

The above Eqs. (10) and (11) can be proved by the pH decrease at the end of every stage in Fig. 4(a).

5. Conclusions

In this study, a series of lab-scale experiments was conducted on bentonite-amended Fukakusa clay to evaluate the membrane behavior towards heavy metals zinc and lead. The chemico-osmotic efficiency coefficient, ω, was obtained in Zn(II) and Pb(II) solutions with concentrations of 0.5, 1, 5, 10, and 50 mM. According to the results, the membrane behavior decreased as the concentration increased, which is consistent with the Gouy-Chapman theory. The bentonite was also found unable to swell sufficiently under relatively high concentrations of Zn(II) and Pb(II), which was proven by SEM images. This observation can help elaborate the decrease of membrane behavior as concentration increases. Compared to normal inorganic ions, the membrane behavior towards heavy metal ions was lower. According to the XRF and XRD results, it can also be concluded that ion exchange reaction or adsorption towards Zn(II) and Pb(II) have occurred, which can restrict the migrations of heavy metal ions.

Acknowledgments

The research presented herein is supported by the Japan Society for the Promotion of Science (JSPS) through a Grant-in-Aid for Scientific Research (Grant No. 22360185), National Natural Science Foundation of China (Grant 51308310), Zhejiang Provincial Natural Science Foundation of China (Grant LQ13E080007), and by the Scientific Research Foundation for the Returned Overseas Chinese Scholars (Chinese State Education Ministry).

References

Barbour, S.L. and Fredlund, D.G. (1989), “Mechanisms of osmotic flow and volume change in clay soils”, *Can. Geotech. J.*, **26**(4), 551-562.

Baun, D.L. and Christensen, T.H. (2004), “Speciation of heavy metals in landfill leachate: A review”, *Waste Manage. Res.*, **22**(1), 3-23.

Canadian Water Quality Guidelines (2004), Guidelines for Canadian drinking water quality, January 8th,

2014. www.worldcat.org/identities/lccn-n82-136902

Chapuis, R.P. (2002), "The 2000 R.M. Hardy Lecture: Full-scale hydraulic performance of soil–bentonite and compacted clay liners", *Can. Geotech. J.*, **39**(2), 417-439.

Dominijanni, A. and Manassero, M. (2012a), "Modelling the swelling and osmotic properties of clay soils. Part I: The phenomenological approach", *Int. J. Eng. Sci.*, **51**, 32-50.

Dominijanni, A. and Manassero, M. (2012b), "Modelling the swelling and osmotic properties of clay soils. Part II: The physical approach", *Int. J. Eng. Sci.*, **51**, 51-73.

Groenevelt, P.H. and Elrick, D.E. (1976), "Coupling phenomena in saturated homo-ionic montmorillonite: II. Theoretical", *Soil Sci. Soc. Am. J.*, **40**(6), 820-823.

Hong, S.M., Candelone, J.P., Patterson, C.C. and Boutron, C.F. (1994), "Greenland ice evidence of hemispheric lead pollution two millennia ago by Greek and Roman civilizations", *Science*, **265**(5180), 1841-1843.

Indian Standard (1991), Drinking water—Specification (First revision); Indian Standard 10500, New Delhi, India.

Kamon, M. and Katsumi, T. (2001), *Clay Liners for Waste Landfill*, Clay Science for Engineering, Balkema, Rotterdam, Netherlands, pp. 29-45.

Kang, J.B. and Shackelford, C.D. (2009), "Clay membrane testing using a flexible-wall cell under closed-system boundary conditions", *Appl. Clay Sci.*, **44**(1-2), 43-58.

Kang, J.B. and Shackelford, C.D. (2010), "Membrane behavior of compacted clay liners", *J. Geotech. Geoenviron. Eng. (ASCE)*, **136**(10), 1368-1382.

Kang, J.B. and Shackelford, C.D. (2011), "Consolidation enhanced membrane behavior of a geosynthetic clay liner", *Geotext. Geomembr.*, **29**(6), 544-556.

Katchalsky, A. and Curran, P.F. (1965), *Nonequilibrium Thermodynamics in Bophysics*, Harvard University Press, Cambridge, MA, USA.

Katsumi, T., Ishimori, H., Ogawa, A., Yoshikawa, K., Hanamoto, K. and Fukagawa, R. (2007), "Hydraulic conductivity of nonprehydrated geosynthetic clay liners permeated with inorganic solutions and waste leachates", *Soil Found.*, **47**(1), 79-96.

Katsumi, T., Ishimori, H., Ogawa, A., Maruyama, S. and Fukagawa, R. (2008a), "Effects of water content distribution on hydraulic conductivity of prehydrated FCLs against calcium chloride solutions", *Soil Found.*, **48**(3), 407-417.

Katsumi, T., Ishimori, H., Onikata, M. and Fukagawa, R. (2008b), "Long-term barrier performance of modified bentonite materials against sodium and calcium permeant solutions", *Geotext. Geomembr.*, **26**(1), 14-30.

Keijzer, T.J.S., Kleingeld, P.J. and Loch, J.P.G. (1997), "Chemical osmosis in compacted clayey material and the prediction of water transport", *Geoenvironmental Engineering, Contaminated Ground: Fate of Pollutants and Remediation*, (R.N. Yong and H.R. Thomas Eds.), Thomas Telford, London, UK, pp. 199-204.

Kemper, W.D. and Rollins, J.B. (1966), "Osmotic efficiency coefficients across compacted clays", *Soil Sci. Soc. Am. Proceedings*, **30**(5), 529-534.

Kimbrough, D.E. and Suffer, I.H. (1995), "Off-site forensic determinations of airborne elemental emissions by multimedia analysis − A case study at 2 secondary lead smelters", *Environ. Sci. Technol.*, **29**(9), 2217-2221.

Malusis, M.A. and Shackelford, C.D. (2002), "Chemico-osmotic efficiency of a geosynthetic clay liner", *J. Geotech. Geoenviro. Eng. (ASCE)*, **128**(2), 97-106.

Malusis, M.A., Shackelford, C.D. and Olsen, H.W. (2001), "A laboratory apparatus to measure chemico-osmotic efficiency coefficients for clay soils", *Geotech. Test. J.*, **24**(3), 229-242.

Manassero, M. and Dominijanni, A. (2003), "Modelling the osmosis effect on solute migration through porous media", *Geotechnique*, **53**(5), 481-492.

Metten, U. (1966), *Desalination by Reverse Osmosis*, M.I.T. Press, Cambridge, MA, USA.

Mitchell, J.K. (1993), *Fundamentals of Soil Behavior*, (2nd Ed.), Wiley, New York, NY, USA.

Olsen, H.W. (1969), "Simultaneous fluxes of liquid and charge in saturated kaolinite", *Soil Sci. Soc. Am.*

Proceedings, **33**(3), 338-344.

Olsen, H.W., Yearsley, E.N. and Nelson, K.R. (1990), "Chemico-osmosis versus diffusion-osmosis". *Transportation Research Record*, 1288, Washington D.C., USA, pp. 15-22.

Shackelford, C.D., Benson, C.H., Katsumi, T., Edil, T.B. and Lin, L. (2000), "Evaluating the hydraulic conductivity of GCLs permeated with non-standard liquids", *Geotext. Geomembr.*, **18**(2-4), 133-161.

Shackelford, C.D. (2012), "Membrane behavior of engineered clay barriers for geoenvironmental containment: state-of-the-art", *Proceedings of GeoCongress 2012: State of the Art and Practice in Geotechnical Engineering*, Geotechnical Special Publication 225; Oakland, CA, USA, March, pp. 3419-3428.

Shelley, T. and Daniel, D. (1993), "Effect of gravel on hydraulic conductivity of compacted soil liners", *J. Geotech. Geoenviron. Eng. (ASCE)*, **119**(1), 54-68.

Sposito, G. (1984), *The Surface Chemistry of Soils*, Oxford University Press, New York, NY, USA.

Tang, Q., Tang, X.W., Li, Z.Z., Chen, Y.M., Kou, N.Y. and Sun, Z.F. (2009), "Adsorption and desorption behaviour of Pb(II) on a natural kaolin: equilibrium, kinetic and thermodynamic studies", *J. Chem. Technol. Biotechnol.*, **84**(9), 1371-1380.

Tang, Q., Tang, X.W., Hu, M.M., Li, Z.Z., Chen, Y.M. and Lou, P. (2010), "Removal of Cd(II) from aqueous solution with activated Firmiana Simplex Leaf: Behaviors and affecting factors", *J. Hazard. Mater.*, **179**(1-3), 95-103.

Tang, Q., Tang, X.W., Li, Z.Z., Wang, Y., Hu, M.M., Zhang, X.J. and Chen, Y.M. (2012), "Zn(II) Removal with Activated Firmiana Simplex Leaf: Kinetics and Equilibrium Studies", *J. Environ. Eng. (ASCE)*, **138**(2), 190-199.

Tang, Q., Katsumi, T., Inui, T. and Li, Z.Z. (2014), "Membrane behavior of bentonite-amended compacted clay", *Soil. Found.*, **54**(3), 329-344.

Tang, Q., Katsumi, T., Inui, T. and Li, Z.Z. (2015), "Influence of pH on the membrane behavior of bentonite amended Fukakusa clay", *Separ. Purif. Technol.*, **141**, 132-142.

Tinoco, I., Sauer, K. and Wang, J.C. (1995), *Physical Chemistry*, Prentice-Hall, Upper Saddle River, NJ, USA.

U.S. EPA (2011), US EPA Drinking Water Standards and Health Advisories; EPA 820-R-11-002. U.S. Environmental Protection Agency, Washington, D.C., USA.

Van Impe, P.O. (2002), "Consolidation, contaminant transport and chemico-osmotic effects in liner materials, A theoretical and experimental study", Doctor Thesis.

Van, O.E., Hale, A.H., Mody, F.K. and Roy, S. (1996), "Transport in shales and the design of improved water-based shale drilling fluids", *SPEDC*, **11**(3), 137-146.

World Health Organization (WHO) (2006), "Guidelines for drinking-water quality: Incorporating first addendum", Vol. 1, Recommendations, World Health Organization, Geneva, Switzerland.

Yaroshchuk, A.E. (1995), "Osmosis and reverse osmosis in fine-charged diaphragms and membranes", *Adv. Colloid Interf. Sci.*, **60**(1-2), 1-93.

Yong, R.N., Pusch, R. and Nakano, M. (2010), *Containment of High-level Radioactive and Hazardous Solid Wastes with Clay Barriers*, Spon Press, Taylor & Francis, London and New York.

RJ